Precise Measurement of the $e^+e^- \to D_s^{*+}D_s^{*-}$ Cross Sections at Center-of-Mass Energies from Threshold to 4.95 GeV

M. Ablikim,[1] M. N. Achasov,[5,b] P. Adlarson,[75] X. C. Ai,[81] R. Aliberti,[36] A. Amoroso,[74a,74c] M. R. An,[40] Q. An,[71,58] Y. Bai,[57] O. Bakina,[37] I. Balossino,[30a] Y. Ban,[47,g] V. Batozskaya,[1,45] K. Begzsuren,[33] N. Berger,[36] M. Berlowski,[45] M. Bertani,[29a] D. Bettoni,[30a] F. Bianchi,[74a,74c] E. Bianco,[74a,74c] A. Bortone,[74a,74c] I. Boyko,[37] R. A. Briere,[6] A. Brueggemann,[68] H. Cai,[76] X. Cai,[1,58] A. Calcaterra,[29a] G. F. Cao,[1,63] N. Cao,[1,63] S. A. Cetin,[62a] J. F. Chang,[1,58] T. T. Chang,[77] W. L. Chang,[1,63] G. R. Che,[44] G. Chelkov,[37,a] C. Chen,[44] Chao Chen,[55] G. Chen,[1] H. S. Chen,[1,63] M. L. Chen,[1,58,63] S. J. Chen,[43] S. M. Chen,[61] T. Chen,[1,63] X. R. Chen,[32,63] X. T. Chen,[1,63] Y. B. Chen,[1,58] Y. Q. Chen,[35] Z. J. Chen,[26,h] W. S. Cheng,[74c] S. K. Choi,[11] X. Chu,[44] G. Cibinetto,[30a] S. C. Coen,[4] F. Cossio,[74c] J. J. Cui,[50] H. L. Dai,[1,58] J. P. Dai,[79] A. Dbeyssi,[19] R. E. de Boer,[4] D. Dedovich,[37] Z. Y. Deng,[1] A. Denig,[36] I. Denysenko,[37] M. Destefanis,[74a,74c] F. De Mori,[74a,74c] B. Ding,[66,1] X. X. Ding,[47,g] Y. Ding,[41] Y. Ding,[35] J. Dong,[1,58] L. Y. Dong,[1,63] M. Y. Dong,[1,58,63] X. Dong,[76] M. C. Du,[1] S. X. Du,[81] Z. H. Duan,[43] P. Egorov,[37,a] Y. L. Fan,[76] J. Fang,[1,58] S. S. Fang,[1,63] W. X. Fang,[1] Y. Fang,[1] R. Farinelli,[30a] L. Fava,[74b,74c] F. Feldbauer,[4] G. Felici,[29a] C. Q. Feng,[71,58] J. H. Feng,[59] K. Fischer,[69] M. Fritsch,[4] C. Fritzsch,[68] C. D. Fu,[1] J. L. Fu,[63] Y. W. Fu,[1] H. Gao,[63] Y. N. Gao,[47,g] Yang Gao,[71,58] S. Garbolino,[74c] I. Garzia,[30a,30b] P. T. Ge,[76] Z. W. Ge,[43] C. Geng,[59] E. M. Gersabeck,[67] A. Gilman,[69] K. Goetzen,[14] L. Gong,[41] W. X. Gong,[1,58] W. Gradl,[36] S. Gramigna,[30a,30b] M. Greco,[74a,74c] M. H. Gu,[1,58] Y. T. Gu,[16] C. Y. Guan,[1,63] Z. L. Guan,[23] A. Q. Guo,[32,63] L. B. Guo,[42] M. J. Guo,[50] R. P. Guo,[49] Y. P. Guo,[13,f] A. Guskov,[37,a] T. T. Han,[50] W. Y. Han,[40] X. Q. Hao,[20] F. A. Harris,[65] K. K. He,[55] K. L. He,[1,63] F. H. H. Heinsius,[4] C. H. Heinz,[36] Y. K. Heng,[1,58,63] C. Herold,[60] T. Holtmann,[4] P. C. Hong,[13,f] G. Y. Hou,[1,63] X. T. Hou,[1,63] Y. R. Hou,[63] Z. L. Hou,[1] H. M. Hu,[1,63] J. F. Hu,[56,i] T. Hu,[1,58,63] Y. Hu,[1] G. S. Huang,[71,58] K. X. Huang,[59] L. Q. Huang,[32,63] X. T. Huang,[50] Y. P. Huang,[1] T. Hussain,[73] N. Hüsken,[28,36] W. Imoehl,[28] M. Irshad,[71,58] J. Jackson,[28] S. Jaeger,[4] S. Janchiv,[33] J. H. Jeong,[11] Q. Ji,[1] Q. P. Ji,[20] X. B. Ji,[1,63] X. L. Ji,[1,58] Y. Y. Ji,[50] X. Q. Jia,[50] Z. K. Jia,[71,58] P. C. Jiang,[47,g] S. S. Jiang,[40] T. J. Jiang,[17] X. S. Jiang,[1,58,63] Y. Jiang,[63] J. B. Jiao,[50] Z. Jiao,[24] S. Jin,[43] Y. Jin,[66] M. Q. Jing,[1,63] T. Johansson,[75] X. K.,[1] S. Kabana,[34] N. Kalantar-Nayestanaki,[64] X. L. Kang,[10] X. S. Kang,[41] R. Kappert,[64] M. Kavatsyuk,[64] B. C. Ke,[81] A. Khoukaz,[68] R. Kiuchi,[1] R. Kliemt,[14] O. B. Kolcu,[62a] B. Kopf,[4] M. K. Kuessner,[4] A. Kupsc,[45,75] W. Kühn,[38] J. J. Lane,[67] P. Larin,[19] A. Lavania,[27] L. Lavezzi,[74a,74c] T. T. Lei,[71,k] Z. H. Lei,[71,58] H. Leithoff,[36] M. Lellmann,[36] T. Lenz,[36] C. Li,[44] C. Li,[48] C. H. Li,[40] Cheng Li,[71,58] D. M. Li,[81] F. Li,[1,58] G. Li,[1] H. Li,[71,58] H. B. Li,[1,63] H. J. Li,[20] H. N. Li,[56,i] Hui Li,[44] J. R. Li,[61] J. S. Li,[59] J. W. Li,[50] K. L. Li,[20] Ke Li,[1] L. J. Li,[1,63] L. K. Li,[1] Lei Li,[3] M. H. Li,[44] P. R. Li,[39,j,k] Q. X. Li,[50] S. X. Li,[13] T. Li,[50] W. D. Li,[1,63] W. G. Li,[1] X. H. Li,[71,58] X. L. Li,[50] Xiaoyu Li,[1,63] Y. G. Li,[47,g] Z. J. Li,[59] Z. X. Li,[16] C. Liang,[43] H. Liang,[1,63] H. Liang,[35] H. Liang,[71,58] Y. F. Liang,[54] Y. T. Liang,[32,63] G. R. Liao,[15] L. Z. Liao,[50] Y. P. Liao,[1,63] J. Libby,[27] A. Limphirat,[60] D. X. Lin,[32,63] T. Lin,[1] B. J. Liu,[1] B. X. Liu,[76] C. Liu,[35] C. X. Liu,[1] F. H. Liu,[53] Fang Liu,[1] Feng Liu,[7] G. M. Liu,[56,i] H. Liu,[39,j,k] H. B. Liu,[16] H. M. Liu,[1,63] Huanhuan Liu,[1] Huihui Liu,[22] J. B. Liu,[71,58] J. L. Liu,[72] J. Y. Liu,[1,63] K. Liu,[1] K. Y. Liu,[41] Ke Liu,[23] L. Liu,[71,58] L. C. Liu,[44] Lu Liu,[44] M. H. Liu,[13,f] P. L. Liu,[1] Q. Liu,[63] S. B. Liu,[71,58] T. Liu,[13,f] W. K. Liu,[44] W. M. Liu,[71,58] X. Liu,[39,j,k] Y. Liu,[81] Y. Liu,[39,j,k] Y. B. Liu,[44] Z. A. Liu,[1,58,63] Z. Q. Liu,[50] X. C. Lou,[1,58,63] F. X. Lu,[59] H. J. Lu,[24] J. G. Lu,[1,58] X. L. Lu,[1] Y. Lu,[8] Y. P. Lu,[1,58] Z. H. Lu,[1,63] C. L. Luo,[42] M. X. Luo,[80] T. Luo,[13,f] X. L. Luo,[1,58] X. R. Lyu,[63] Y. F. Lyu,[44] F. C. Ma,[41] H. L. Ma,[1] J. L. Ma,[1,63] L. L. Ma,[50] M. M. Ma,[1,63] Q. M. Ma,[1] R. Q. Ma,[1,63] R. T. Ma,[63] X. Y. Ma,[1,58] Y. Ma,[47,g] Y. M. Ma,[32] F. E. Maas,[19] M. Maggiora,[74a,74c] S. Malde,[69] Q. A. Malik,[73] A. Mangoni,[29b] Y. J. Mao,[47,g] Z. P. Mao,[1] S. Marcello,[74a,74c] Z. X. Meng,[66] J. G. Messchendorp,[14,64] G. Mezzadri,[30a] H. Miao,[1,63] T. J. Min,[43] R. E. Mitchell,[28] X. H. Mo,[1,58,63] N. Yu. Muchnoi,[5,b] Y. Nefedov,[37] F. Nerling,[19,d] I. B. Nikolaev,[5,b] Z. Ning,[1,58] S. Nisar,[12,l] Y. Niu,[50] S. L. Olsen,[63] Q. Ouyang,[1,58,63] S. Pacetti,[29b,29c] X. Pan,[55] Y. Pan,[57] A. Pathak,[35] P. Patteri,[29a] Y. P. Pei,[71,58] M. Pelizaeus,[4] H. P. Peng,[71,58] K. Peters,[14,d] J. L. Ping,[42] R. G. Ping,[1,63] S. Plura,[36] S. Pogodin,[37] V. Prasad,[34] F. Z. Qi,[1] H. Qi,[71,58] H. R. Qi,[61] M. Qi,[43] T. Y. Qi,[13,f] S. Qian,[1,58] W. B. Qian,[63] C. F. Qiao,[63] J. J. Qin,[72] L. Q. Qin,[15] X. P. Qin,[13,f] X. S. Qin,[50] Z. H. Qin,[1,58] J. F. Qiu,[1] S. Q. Qu,[61] C. F. Redmer,[36] K. J. Ren,[40] A. Rivetti,[74c] V. Rodin,[64] M. Rolo,[74c] G. Rong,[1,63] Ch. Rosner,[19] S. N. Ruan,[44] N. Salone,[45] A. Sarantsev,[37,c] Y. Schelhaas,[36] K. Schoenning,[75] M. Scodeggio,[30a,30b] K. Y. Shan,[13,f] W. Shan,[25] X. Y. Shan,[71,58] J. F. Shangguan,[55] L. G. Shao,[1,63] M. Shao,[71,58] C. P. Shen,[13,f] H. F. Shen,[1,63] W. H. Shen,[63] X. Y. Shen,[1,63] B. A. Shi,[63] H. C. Shi,[71,58] J. L. Shi,[13] J. Y. Shi,[1] Q. Q. Shi,[55] R. S. Shi,[1,63] X. Shi,[1,58] J. J. Song,[20] T. Z. Song,[59] W. M. Song,[35,1]

Y. J. Song,[13] Y. X. Song,[47,g] S. Sosio,[74a,74c] S. Spataro,[74a,74c] F. Stieler,[36] Y. J. Su,[63] G. B. Sun,[76] G. X. Sun,[1] H. Sun,[63] H. K. Sun,[1] J. F. Sun,[20] K. Sun,[61] L. Sun,[76] S. S. Sun,[1,63] T. Sun,[1,63] W. Y. Sun,[35] Y. Sun,[10] Y. J. Sun,[71,58] Y. Z. Sun,[1] Z. T. Sun,[50] Y. X. Tan,[71,58] C. J. Tang,[54] G. Y. Tang,[1] J. Tang,[59] Y. A. Tang,[76] L. Y. Tao,[72] Q. T. Tao,[26,h] M. Tat,[69] J. X. Teng,[71,58] V. Thoren,[75] W. H. Tian,[52] W. H. Tian,[59] Y. Tian,[32,63] Z. F. Tian,[76] I. Uman,[62b] S. J. Wang,[50] B. Wang,[1] B. L. Wang,[63] Bo Wang,[71,58] C. W. Wang,[43] D. Y. Wang,[47,g] F. Wang,[72] H. J. Wang,[39,j,k] H. P. Wang,[1,63] J. P. Wang,[50] K. Wang,[1,58] L. L. Wang,[1] M. Wang,[50] Meng Wang,[1,63] S. Wang,[39,j,k] S. Wang,[13,f] T. Wang,[13,f] T. J. Wang,[44] W. Wang,[59] W. Wang,[72] W. P. Wang,[71,58] X. Wang,[47,g] X. F. Wang,[39,j,k] X. J. Wang,[40] X. L. Wang,[13,f] Y. Wang,[61] Y. D. Wang,[46] Y. F. Wang,[1,58,63] Y. H. Wang,[48] Y. N. Wang,[46] Y. Q. Wang,[1] Yaqian Wang,[18,1] Yi Wang,[61] Z. Wang,[1,58] Z. L. Wang,[72] Z. Y. Wang,[1,63] Ziyi Wang,[63] D. Wei,[70] D. H. Wei,[15] F. Weidner,[68] S. P. Wen,[1] C. W. Wenzel,[4] U. W. Wiedner,[4] G. Wilkinson,[69] M. Wolke,[75] L. Wollenberg,[4] C. Wu,[40] J. F. Wu,[1,63] L. H. Wu,[1] L. J. Wu,[1,63] X. Wu,[13,f] X. H. Wu,[35] Y. Wu,[71] Y. J. Wu,[32] Z. Wu,[1,58] L. Xia,[71,58] X. M. Xian,[40] T. Xiang,[47,g] D. Xiao,[39,j,k] G. Y. Xiao,[43] H. Xiao,[13,f] S. Y. Xiao,[1] Y. L. Xiao,[13,f] Z. J. Xiao,[42] C. Xie,[43] X. H. Xie,[47,g] Y. Xie,[50] Y. G. Xie,[1,58] Y. H. Xie,[7] Z. P. Xie,[71,58] T. Y. Xing,[1,63] C. F. Xu,[1,63] C. J. Xu,[59] G. F. Xu,[1] H. Y. Xu,[66] Q. J. Xu,[17] Q. N. Xu,[31] W. Xu,[1,63] W. L. Xu,[66] X. P. Xu,[55] Y. C. Xu,[78] Z. P. Xu,[43] Z. S. Xu,[63] F. Yan,[13,f] L. Yan,[13,f] W. B. Yan,[71,58] W. C. Yan,[81] X. Q. Yan,[1] H. J. Yang,[51,e] H. L. Yang,[35] H. X. Yang,[1] Tao Yang,[1] Y. Yang,[13,f] Y. F. Yang,[44] Y. X. Yang,[1,63] Yifan Yang,[1,63] Z. W. Yang,[39,j,k] Z. P. Yao,[50] M. Ye,[1,58] M. H. Ye,[9] J. H. Yin,[1] Z. Y. You,[59] B. X. Yu,[1,58,63] C. X. Yu,[44] G. Yu,[1,63] J. S. Yu,[26,h] T. Yu,[72] X. D. Yu,[47,g] C. Z. Yuan,[1,63] L. Yuan,[2] S. C. Yuan,[1] X. Q. Yuan,[1] Y. Yuan,[1,63] Z. Y. Yuan,[59] C. X. Yue,[40] A. A. Zafar,[73] F. R. Zeng,[50] X. Zeng,[13,f] Y. Zeng,[26,h] Y. J. Zeng,[1,63] X. Y. Zhai,[35] Y. C. Zhai,[50] Y. H. Zhan,[59] A. Q. Zhang,[1,63] B. L. Zhang,[1,63] B. X. Zhang,[1] D. H. Zhang,[44] G. Y. Zhang,[20] H. Zhang,[71] H. H. Zhang,[59] H. H. Zhang,[35] H. Q. Zhang,[1,58,63] H. Y. Zhang,[1,58] J. J. Zhang,[52] J. L. Zhang,[21] J. Q. Zhang,[42] J. W. Zhang,[1,58,63] J. X. Zhang,[39,j,k] J. Y. Zhang,[1] J. Z. Zhang,[1,63] Jianyu Zhang,[63] Jiawei Zhang,[1,63] L. M. Zhang,[61] L. Q. Zhang,[59] Lei Zhang,[43] P. Zhang,[1] Q. Y. Zhang,[40,81] Shuihan Zhang,[1,63] Shulei Zhang,[26,h] X. D. Zhang,[46] X. M. Zhang,[1] X. Y. Zhang,[55] X. Y. Zhang,[50] Y. Zhang,[69] Y. Zhang,[72] Y. T. Zhang,[81] Y. H. Zhang,[1,58] Yan Zhang,[71,58] Yao Zhang,[1] Z. H. Zhang,[1] Z. L. Zhang,[35] Z. Y. Zhang,[76] Z. Y. Zhang,[44] G. Zhao,[1] J. Zhao,[40] J. Y. Zhao,[1,63] J. Z. Zhao,[1,58] Lei Zhao,[71,58] Ling Zhao,[1] M. G. Zhao,[44] S. J. Zhao,[81] Y. B. Zhao,[1,58] Y. X. Zhao,[32,63] Z. G. Zhao,[71,58] A. Zhemchugov,[37,a] B. Zheng,[72] J. P. Zheng,[1,58] W. J. Zheng,[1,63] Y. H. Zheng,[63] B. Zhong,[42] X. Zhong,[59] H. Zhou,[50] L. P. Zhou,[1,63] X. Zhou,[76] X. K. Zhou,[7] X. R. Zhou,[71,58] X. Y. Zhou,[40] Y. Z. Zhou,[13,f] J. Zhu,[44] K. Zhu,[1] K. J. Zhu,[1,58,63] L. Zhu,[35] L. X. Zhu,[63] S. H. Zhu,[70] S. Q. Zhu,[43] T. J. Zhu,[13,f] W. J. Zhu,[13,f] Y. C. Zhu,[71,58] Z. A. Zhu,[1,63] J. H. Zou,[1] and J. Zu[71,58]

(BESIII Collaboration)

[1]*Institute of High Energy Physics, Beijing 100049, People's Republic of China*
[2]*Beihang University, Beijing 100191, People's Republic of China*
[3]*Beijing Institute of Petrochemical Technology, Beijing 102617, People's Republic of China*
[4]*Bochum Ruhr-University, D-44780 Bochum, Germany*
[5]*Budker Institute of Nuclear Physics SB RAS (BINP), Novosibirsk 630090, Russia*
[6]*Carnegie Mellon University, Pittsburgh, Pennsylvania 15213, USA*
[7]*Central China Normal University, Wuhan 430079, People's Republic of China*
[8]*Central South University, Changsha 410083, People's Republic of China*
[9]*China Center of Advanced Science and Technology, Beijing 100190, People's Republic of China*
[10]*China University of Geosciences, Wuhan 430074, People's Republic of China*
[11]*Chung-Ang University, Seoul, 06974, Republic of Korea*
[12]*COMSATS University Islamabad, Lahore Campus, Defence Road, Off Raiwind Road, 54000 Lahore, Pakistan*
[13]*Fudan University, Shanghai 200433, People's Republic of China*
[14]*GSI Helmholtzcentre for Heavy Ion Research GmbH, D-64291 Darmstadt, Germany*
[15]*Guangxi Normal University, Guilin 541004, People's Republic of China*
[16]*Guangxi University, Nanning 530004, People's Republic of China*
[17]*Hangzhou Normal University, Hangzhou 310036, People's Republic of China*
[18]*Hebei University, Baoding 071002, People's Republic of China*
[19]*Helmholtz Institute Mainz, Staudinger Weg 18, D-55099 Mainz, Germany*
[20]*Henan Normal University, Xinxiang 453007, People's Republic of China*
[21]*Henan University, Kaifeng 475004, People's Republic of China*
[22]*Henan University of Science and Technology, Luoyang 471003, People's Republic of China*
[23]*Henan University of Technology, Zhengzhou 450001, People's Republic of China*

[24]*Huangshan College, Huangshan 245000, People's Republic of China*
[25]*Hunan Normal University, Changsha 410081, People's Republic of China*
[26]*Hunan University, Changsha 410082, People's Republic of China*
[27]*Indian Institute of Technology Madras, Chennai 600036, India*
[28]*Indiana University, Bloomington, Indiana 47405, USA*
[29a]*INFN Laboratori Nazionali di Frascati, INFN Laboratori Nazionali di Frascati, I-00044, Frascati, Italy*
[29b]*INFN Sezione di Perugia, I-06100, Perugia, Italy*
[29c]*University of Perugia, I-06100, Perugia, Italy*
[30a]*INFN Sezione di Ferrara, INFN Sezione di Ferrara, I-44122, Ferrara, Italy*
[30b]*University of Ferrara, I-44122, Ferrara, Italy*
[31]*Inner Mongolia University, Hohhot 010021, People's Republic of China*
[32]*Institute of Modern Physics, Lanzhou 730000, People's Republic of China*
[33]*Institute of Physics and Technology, Peace Avenue 54B, Ulaanbaatar 13330, Mongolia*
[34]*Instituto de Alta Investigación, Universidad de Tarapacá, Casilla 7D, Arica 1000000, Chile*
[35]*Jilin University, Changchun 130012, People's Republic of China*
[36]*Johannes Gutenberg University of Mainz, Johann-Joachim-Becher-Weg 45, D-55099 Mainz, Germany*
[37]*Joint Institute for Nuclear Research, 141980 Dubna, Moscow region, Russia*
[38]*Justus-Liebig-Universitaet Giessen, II. Physikalisches Institut, Heinrich-Buff-Ring 16, D-35392 Giessen, Germany*
[39]*Lanzhou University, Lanzhou 730000, People's Republic of China*
[40]*Liaoning Normal University, Dalian 116029, People's Republic of China*
[41]*Liaoning University, Shenyang 110036, People's Republic of China*
[42]*Nanjing Normal University, Nanjing 210023, People's Republic of China*
[43]*Nanjing University, Nanjing 210093, People's Republic of China*
[44]*Nankai University, Tianjin 300071, People's Republic of China*
[45]*National Centre for Nuclear Research, Warsaw 02-093, Poland*
[46]*North China Electric Power University, Beijing 102206, People's Republic of China*
[47]*Peking University, Beijing 100871, People's Republic of China*
[48]*Qufu Normal University, Qufu 273165, People's Republic of China*
[49]*Shandong Normal University, Jinan 250014, People's Republic of China*
[50]*Shandong University, Jinan 250100, People's Republic of China*
[51]*Shanghai Jiao Tong University, Shanghai 200240, People's Republic of China*
[52]*Shanxi Normal University, Linfen 041004, People's Republic of China*
[53]*Shanxi University, Taiyuan 030006, People's Republic of China*
[54]*Sichuan University, Chengdu 610064, People's Republic of China*
[55]*Soochow University, Suzhou 215006, People's Republic of China*
[56]*South China Normal University, Guangzhou 510006, People's Republic of China*
[57]*Southeast University, Nanjing 211100, People's Republic of China*
[58]*State Key Laboratory of Particle Detection and Electronics, Beijing 100049, Hefei 230026, People's Republic of China*
[59]*Sun Yat-Sen University, Guangzhou 510275, People's Republic of China*
[60]*Suranaree University of Technology, University Avenue 111, Nakhon Ratchasima 30000, Thailand*
[61]*Tsinghua University, Beijing 100084, People's Republic of China*
[62a]*Turkish Accelerator Center Particle Factory Group, Istinye University, 34010, Istanbul, Turkey*
[62b]*Near East University, Nicosia, North Cyprus, 99138, Mersin 10, Turkey*
[63]*University of Chinese Academy of Sciences, Beijing 100049, People's Republic of China*
[64]*University of Groningen, NL-9747 AA Groningen, The Netherlands*
[65]*University of Hawaii, Honolulu, Hawaii 96822, USA*
[66]*University of Jinan, Jinan 250022, People's Republic of China*
[67]*University of Manchester, Oxford Road, Manchester, M13 9PL, United Kingdom*
[68]*University of Muenster, Wilhelm-Klemm-Strasse 9, 48149 Muenster, Germany*
[69]*University of Oxford, Keble Road, Oxford OX13RH, United Kingdom*
[70]*University of Science and Technology Liaoning, Anshan 114051, People's Republic of China*
[71]*University of Science and Technology of China, Hefei 230026, People's Republic of China*
[72]*University of South China, Hengyang 421001, People's Republic of China*
[73]*University of the Punjab, Lahore-54590, Pakistan*
[74a]*University of Turin and INFN, University of Turin, I-10125, Turin, Italy*
[74b]*University of Eastern Piedmont, I-15121, Alessandria, Italy*
[74c]*INFN, I-10125, Turin, Italy*
[75]*Uppsala University, Box 516, SE-75120 Uppsala, Sweden*
[76]*Wuhan University, Wuhan 430072, People's Republic of China*

[77]Xinyang Normal University, Xinyang 464000, People's Republic of China
[78]Yantai University, Yantai 264005, People's Republic of China
[79]Yunnan University, Kunming 650500, People's Republic of China
[80]Zhejiang University, Hangzhou 310027, People's Republic of China
[81]Zhengzhou University, Zhengzhou 450001, People's Republic of China

(Received 19 May 2023; revised 16 August 2023; accepted 29 August 2023; published 13 October 2023)

The process $e^+e^- \to D_s^{*+}D_s^{*-}$ is studied with a semi-inclusive method using data samples at center-of-mass energies from threshold to 4.95 GeV collected with the BESIII detector operating at the Beijing Electron Positron Collider. The Born cross sections of the process are measured for the first time with high precision in this energy region. Two resonance structures are observed in the energy-dependent cross sections around 4.2 and 4.4 GeV. By fitting the cross sections with a coherent sum of three Breit-Wigner amplitudes and one phase-space amplitude, the two significant structures are assigned masses of $(4186.8 \pm 8.7 \pm 30)$ and $(4414.6 \pm 3.4 \pm 6.1)$ MeV$/c^2$, widths of $(55 \pm 15 \pm 53)$ and $(122.5 \pm 7.5 \pm 8.1)$ MeV, where the first errors are statistical and the second ones are systematic. The inclusion of a third Breit-Wigner amplitude is necessary to describe a structure around 4.79 GeV.

DOI: 10.1103/PhysRevLett.131.151903

In e^+e^- annihilations, several conventional vector charmonium states are established in the inclusive hadronic cross sections above the open charm threshold, such as the $\psi(3770)$, $\psi(4040)$, $\psi(4160)$, and $\psi(4415)$. However, unexpected vector charmoniumlike resonance structures have also been discovered over the past two decades with a charmonium and light hadrons in the final state. These include $\psi(4230)$, initially observed in the $e^+e^- \to \pi^+\pi^- J/\psi$ process [1,2], and $\psi(4360)$ and $\psi(4660)$, initially observed in $e^+e^- \to \pi^+\pi^-\psi(3686)$ [3,4] by the B-factory experiments *BABAR* and Belle.

These vector charmonium(-like) states have been searched for or further investigated experimentally in many decay modes, involving charmonium states (such as $\pi^+\pi^- J/\psi$ [5], $K\bar{K}J/\psi$ [6,7], $\eta J/\psi$ [8,9], $\eta' J/\psi$ [10], $\pi\pi h_c$ [11–13], $\pi^+\pi^-\psi(3686)$ [14], and $\omega\chi_{cJ}$ [15]), and charmed mesons (such as $D\bar{D}$ [16,17], $D^{*0}D^{*-}\pi^+ + \text{c.c.}$ [18] and $\bar{D}D^*\pi + \text{c.c.}$ [19]), whereas experimental results of the decay modes involving charmed strange mesons are inadequate. Interestingly, the mass of the $\psi(4230)$ state lies just at the production threshold of the $D_s^{*+}D_s^{*-}$ pair.

The measurements of the exclusive cross sections for charmed strange meson pairs were performed by CLEO-c at center-of-mass energies ($E_{\text{c.m.}}$) up to 4.26 GeV [20], and by *BABAR* [21] and Belle [22] with the initial-state radiation (ISR) method. Since these results are limited by either energy range (CLEO-c) or statistics (*BABAR* and Belle), it could not be concluded yet whether these vector charmonium(-like) states decay into charmed strange meson pairs or not.

With the data samples taken by the BESIII experiment, the cross sections of $e^+e^- \to D_s^{*+}D_s^{*-}$ can be measured from the production threshold up to 4.95 GeV, with much improved precision over previous experiments. This unique measurement allows to investigate the vector chamonium(-like) structures, therefore shedding light on their nature.

The BESIII detector is described in detail in [23,24]. The experimental data used in this analysis were taken at $E_{\text{c.m.}}$ ranging from 4.226 GeV (just above the $D_s^{*+}D_s^{*-}$ production threshold) to 4.95 GeV with 76 energy points [25–27] corresponding in total to an integrated luminosity of 15.67 fb^{-1} [27–29]. A Geant4-based [30] Monte Carlo (MC) package, which includes the geometric description of the BESIII detector and its response, is used to produce simulated samples which are used to estimate the backgrounds and to determine the detection efficiencies and ISR corrections.

The $e^+e^- \to D_s^{*+}D_s^{*-}$ events are generated using helicity-amplitude (HELAMP) models in EvtGen [31,32] at all the energy points, where the HELAMP inputs (relative magnitudes of the helicity amplitudes) are extracted from the helicity angular distributions of data, the width of $D_s^{*\pm}$ is set to zero, and beam energy spread and ISR are considered with the generator KKMC [33,34]. Possible background contributions are estimated with inclusive MC samples generated by KKMC with integrated luminosities comparable to data, in which the known decay modes are modeled with EvtGen using branching fractions taken from the Particle Data Group [35], and the remaining unknown charmonium decays are modeled with LUNDCHARM [36]. Final-state radiation (FSR) from charged particles is incorporated by the PHOTOS package [37].

To increase efficiency, a semi-inclusive method is performed by reconstructing only D_s^{*+} or D_s^{*-} of $e^+e^- \to D_s^{*+}D_s^{*-}$, with $D_s^{*\pm} \to \gamma D_s^\pm \to \gamma K^+K^-\pi^\pm$. With this method at least one good photon, one pair of K^+K^-, and one $\pi^\pm$ are required in the final state. The selection criteria for charged tracks and photon candidates are described in Ref. [38]. To select $D_s^\pm$ candidates, the invariant mass $m_{KK\pi}$ of $K^+K^-\pi^\pm$ is required to be in the range $|m_{KK\pi} - m_{D_s}| < 15$ MeV$/c^2$, where m_{D_s} is the nominal $D_s^\pm$ mass [35]. All the $\gamma D_s^\pm$ (i.e. $\gamma K^+K^-\pi^\pm$) combinations are taken as $D_s^{*\pm}$ candidates for further selection. As the missing mass $m_{\rm miss}$ and the invariant mass $m_{\gamma KK\pi}$ of $D_s^{*\pm} \to \gamma K^+K^-\pi^\pm$ candidates are anticorrelated, a modified missing mass $M_{\rm miss} \equiv m_{\rm miss} + m_{\gamma KK\pi} - m_{D_s^*}$ is used to improve the resolution, where $m_{D_s^*}$ is the nominal mass of $D_s^{*\pm}$ [35]. With the signal MC events, the resolution of $M_{\rm miss}$ is estimated and parametrized as an energy dependent function $\sigma^{\rm MC}_{M_{\rm miss}}(E_{\rm c.m.})$. To select $D_s^{*\pm}$ from $e^+e^- \to D_s^{*+}D_s^{*-}$ events and suppress background, the modified missing mass of $D_s^{*\pm}$ candidates is required to be in a window $|M_{\rm miss} - m_{D_s^*}| < 5\sigma^{\rm MC}_{M_{\rm miss}}(E_{\rm c.m.})$. Because of the positive correlation between $m_{\gamma KK\pi}$ and $m_{KK\pi}$, a modified mass $M_{\gamma KK\pi} \equiv m_{\gamma KK\pi} - m_{KK\pi} + m_{D_s}$ is used for $D_s^{*\pm}$ candidates to improve the resolution.

The yield of $D_s^{*\pm}$ signals is determined by fitting the $M_{\gamma KK\pi}$ distributions. To describe the $D_s^{*\pm}$ signal shape in data, the $M_{\gamma KK\pi}$ shape of correct $\gamma KK\pi$ combinations from $e^+e^- \to D_s^{*+}D_s^{*-}$ MC, which is figured out by matching the MC truth, is used. This MC signal shape is convolved with a Gaussian function to take into account the possible mass shift Δm, and the resolution (and D_s^* width) difference $\Delta\sigma$ between data and MC simulation. The $M_{\gamma KK\pi}$ shape of random $\gamma KK\pi$ combinations from $e^+e^- \to D_s^{*+}D_s^{*-}$ MC is also used as one component and its ratio relative to the one for correct combinations is fixed according to the MC study. To describe the background in $M_{\gamma KK\pi}$ distribution for data, a second order Chebyshev function $1 + c_0x + c_1(2x^2 - 1)$ with two coefficients c_0 and c_1 is used. The parameters Δm, $\Delta\sigma$, c_0, and c_1 are floating initially in the fits. Since no $E_{\rm c.m.}$ dependence is observed for Δm, $\Delta\sigma$, and c_1, they are finally fixed to the values averaged over $E_{\rm c.m.}$ in the fits to determine the nominal $D_s^{*\pm}$ signal yields, leaving only c_0 as floating. As an example, the fit of $M_{\gamma KK\pi}$ to data at $E_{\rm c.m.} = 4.29$ GeV [39] is shown in Fig. 1.

A study of the inclusive MC samples shows that no peaking background is found from events without $D_s^{*\pm}$ after applying all the selection criteria. The ISR-produced $D_s^\pm D_s^{*\mp}$ events can contribute as a peaking background, which is subtracted by normalized MC according to the cross sections of $e^+e^- \to D_s^\pm D_s^{*\mp}$ [40] and the luminosities. The other two-body processes containing $D_s^{*\pm}$ are $e^+e^- \to D_s^{*\pm}D_{sJ}^{(*)\mp}$, but they fail the missing mass requirement. For the same reason, the three-body process $e^+e^- \to D_s^* D^{(*)} K$ does not contribute as peaking backgrounds either. The contribution from the three-body process $e^+e^- \to D_s^{*\pm}D_s^\mp\pi^0$ is expected to be negligible due to isospin violation and the missing mass requirement.

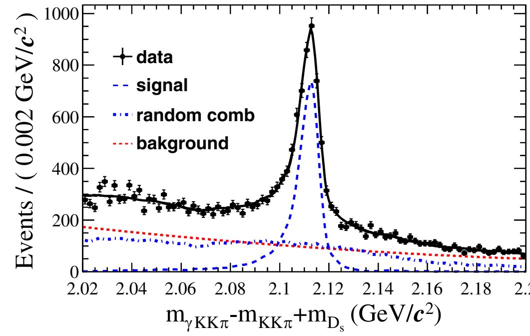

FIG. 1. The $M_{\gamma KK\pi}$ distribution for data at 4.29 GeV. The black curve represents the fit, the red dashed curve the background, the blue dot-dashed curve the random combinations of $\gamma KK\pi$ from $e^+e^- \to D_s^{*\pm}D_s^{*\mp}$, and the blue dashed curve the correct $\gamma KK\pi$ combinations from the signal.

The Born cross section $\sigma_{\rm Born}$ and the dressed cross section $\sigma_{\rm dressed}$ at each energy point are calculated using

$$\sigma_{\rm Born} = \sigma_{\rm dressed}|1-\Pi|^2 = \frac{N^{\rm fit}_{D_s^*} - N_{D_s^\pm D_s^{*\mp}}}{2\mathcal{B}(D_s^\pm \to K^+K^-\pi^\pm)\epsilon(1+\delta)\frac{1}{|1-\Pi|^2}\mathcal{L}_{\rm int}}, \quad (1)$$

where $N^{\rm fit}_{D_s^*}$ is the fitted D_s^* signal yield, $N_{D_s^\pm D_s^{*\mp}}$ is the number of the estimated peaking background events from the ISR produced $D_s^\pm D_s^{*\mp}$, $\mathcal{L}_{\rm int}$ is the integrated luminosity, $1+\delta$ is the ISR correction factor, $(1/|1-\Pi|^2)$ is the correction factor from the vacuum polarization (VP) [41], $\mathcal{B}(D_s^\pm \to K^+K^-\pi^\pm)$ is the branching fraction of the decay $D_s^\pm \to K^+K^-\pi^\pm$, which is taken from Ref. [35], and ϵ is the detection efficiency times the branching fraction of $D_s^{*\pm} \to \gamma D_s^\pm$ [35]. As D_s^{*+} and D_s^{*-} are not separated in the fitted signal yields, there is a factor of 2 in the denominator.

The ISR effect also impacts on the detection efficiency in addition to the correction factor. Since ISR depends on the dressed cross section line shape, an iterative procedure is used to determine the dressed cross sections [42]. First, signal MC samples are generated at all the energy points with a flat dressed cross section line shape using KKMC to determine the initial detection efficiencies, ISR correction factors and subsequently the preliminary measured dressed cross sections. The measured dressed cross sections are fitted with a coherent sum of three Breit-Wigner (BW) and one two-body phase-space (PHSP) amplitudes assuming $D_s^{*+}D_s^{*-}$ in P wave [43]

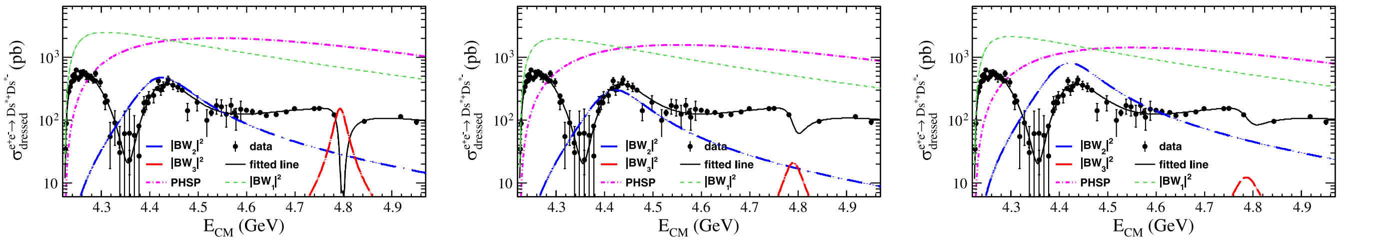

(a) (b) (c)

FIG. 2. Three fitting results for the measured dressed cross sections of $e^+e^- \to D_s^{*+}D_s^{*-}$. The black dots with error bars are for the measured dressed cross sections. In each plot, the black curve represents the fit; the green dashed, blue two-dashed, and red long-dashed ones are for the three BW amplitudes from the fit, respectively, and the pink dot-dashed is for the PHSP contributions.

$$\sigma_{\text{dressed}} = \left| BW_1(E_{\text{c.m.}}) + \sum_{j=2}^{3} BW_j(E_{\text{c.m.}}) e^{i\phi_j} + \frac{a_0\sqrt{\beta^3(E_{\text{c.m.}})}}{E_{\text{c.m.}}^n} e^{i\phi_0} \right|^2, \tag{2}$$

where

$$BW_1(E_{\text{c.m.}}) = \frac{M_1}{E_{\text{c.m.}}} \cdot \frac{B_1(E_{\text{c.m.}})\sqrt{12\pi a_1 \Gamma_1}}{E_{\text{c.m.}}^2 - M_1^2 + iM_1\Gamma_1} \cdot \sqrt{\beta^3(E_{\text{c.m.}})} \tag{3}$$

is the first BW amplitude [44],

$$BW_j(E_{\text{c.m.}}) = \frac{M_j}{E_{\text{c.m.}}} \cdot \frac{B_1(E_{\text{c.m.}})\sqrt{12\pi[\Gamma_{e^+e^-}\text{-}B(D_s^* D_s^*)]_j \Gamma_j}}{E_{\text{c.m.}}^2 - M_j^2 + iM_j\Gamma_j} \cdot \sqrt{\frac{\beta^3(E_{\text{c.m.}})}{\beta^3(M_j)}} \tag{4}$$

is the jth BW amplitude ($j = 2$, 3), the Blatt-Weisskopf function $B_1(E_{\text{c.m.}}) = \sqrt{1/[1 + q^2(E_{\text{c.m.}})R^2]}$ is used as the P-wave barrier factor [45,46] with $q(E_{\text{c.m.}})$ the momentum of $D_s^{*\pm}$ and $R = 1.6\ \text{GeV}^{-1}$ [47] the barrier radius, a_1 is the coefficient for the BW_1, $[\Gamma_{e^+e^-}\text{-}B(D_s^* D_s^*)]_j$ is the product of the e^+e^- partial width and the branching fraction of $D_s^{*+}D_s^{*-}$ for the jth resonance, $\beta(E_{\text{c.m.}})$ is the velocity of $D_s^{*\pm}$, a_0 is the coefficient for the PHSP amplitude, n is a free exponent, ϕ_j and ϕ_0 are the relative phases. With the fitted line shape, a MC-weighting method [42] is used to iteratively update the efficiencies, the ISR correction factors, the measured dressed cross sections, and the fitted line shape. After four iterations, the fit to the measured dressed cross section converged.

TABLE I. The fitting results of the dressed cross sections.

	Result 1	Result 2	Result 3
M_1 (MeV/c^2)	4186.8 ± 8.7	4194.1 ± 6.8	4195.6 ± 6.5
Γ_1 (MeV)	55 ± 15	61.1 ± 8.5	61.7 ± 7.7
M_2 (MeV/c^2)	4414.6 ± 3.4	4411.9 ± 3.2	4411.1 ± 3.2
Γ_2 (MeV)	122.5 ± 7.5	120.2 ± 7.4	119.9 ± 7.3
M_3 (MeV/c^2)	4793.3 ± 6.7	4789.7 ± 8.7	4786.0 ± 9.4
Γ_3 (MeV)	27.1 ± 6.5	42 ± 75	60 ± 34

The final fit of the dressed cross sections of $e^+e^- \to D_s^{*+}D_s^{*-}$ is taken to determine the parameters of the three structures. In the nominal fit of the dressed cross sections, only statistical uncertainties are considered. We find three sets of fitting results with comparable goodness of fit, which are shown in Fig. 2 and Table I. Because of the limited number of data points around 4.79 GeV, the fitted mass of the third structure varies from 4786 to 4793.3 MeV/c^2 and the width from 27.1 to 60 MeV. The statistical significance of the third structure exceeds 5.9σ in all three fitting procedures, indicating that incorporating this amplitude leads to a more accurate description of the cross sections compared to using only two BWs. Besides the three BWs, one additional BW is tried to better describe the data points around 4.55 GeV, but it is not kept due to its small statistical significance.

The Born cross sections are obtained by applying the VP correction on the dressed cross sections. The obtained results are summarized in the Supplemental Material [48]. The systematic uncertainties for the measured Born cross sections are described as follows, some of which are common along all the energy points, while others are estimated depending on the $E_{\text{c.m.}}$ range.

The systematic uncertainties of tracking (particle identification) efficiency are estimated to be 0.5% (0.5%) per

$K^{\pm}$ and 0.2% (0.4%) per $\pi^{\pm}$ with a control sample of $D_s^{\pm} \to K^+K^-\pi^{\pm}$ decays [49]; thus a 1.2% (1.4%) systematic uncertainty is assigned for the tracking efficiency (particle identification) in the $D_s^{\pm} \to K^+K^-\pi^{\pm}$ candidates selection. The systematic uncertainty in the efficiency for photon reconstruction is set conservatively to 1% based on a study with a sample of $J/\psi \to \rho\pi$ events [50]. From fits of the invariant mass spectrum of $D_s^{\pm} \to K^+K^-\pi^{\pm}$ candidates and of the modified missing mass of $D_s^{*\pm} \to \gamma K^+K^-\pi^{\pm}$ candidates, the efficiencies for signal in the mass window for both data and MC samples can be calculated, and the relative differences in efficiency between data and MC simulation are taken as systematic uncertainties for the $D_s^{\pm}$ mass window and the modified missing mass window, respectively, which cover the possible resolution difference and the zero width setting for $D_s^{*\pm}$ in MC simulation. The maximum difference in the dressed cross sections between the last two iterations, 0.2%, is taken as the systematic uncertainty for the stability of the iteration results. The systematic uncertainty of the branching fraction for $D_s^{\pm} \to K^+K^-\pi^{\pm}$ and $D_s^{*\pm} \to \gamma D_s^{\pm}$ is taken from Ref. [35]. The integrated luminosities are measured by QED events [51] with a systematic uncertainty of 1%. The uncertainty from VP correction is 0.1% [41]. The uncertainty of the peaking background subtraction from the $e^+e^- \to D_s^{\pm}D_s^{*\mp}$ process is estimated to be 1% mainly from the uncertainties of cross section measurement. Instead of the HELAMP model, the PHSP model [31,32] is also used to generate $e^+e^- \to D_s^{*\pm}D_s^{*\mp}$ events and the maximum difference in efficiency, 2.2%, is taken as the systematic uncertainty for the generation model. We get the total common systematic uncertainty by adding them in quadrature, which is 4.0%.

The shape related parameters Δm, $\Delta\sigma$, and c_1 are fixed to the averaged values in the nominal fit (see Fig. 1 for an example). The differences of the fitted signal yields, when these parameters are floating, are within statistical uncertainties. However, to cover these differences conservatively, the whole energy range is divided into three intervals (4.226,4.3), (4.3,4.4), and (4.4,4.95) GeV with assigned systematic uncertainties 2%, 5%, and 2%, respectively, due to the signal and background shapes. The boundaries of the nominal fitting range for $M_{\gamma KK\pi}$, which is $[2.02, 2.20]$ GeV/c^2, are changed by 10 MeV to estimate the corresponding fitting range uncertainties. These are assigned to be 4%, 5%, and 4%, respectively, in the energy intervals (4.226,4.3), (4.3,4.4), and (4.4,4.95) GeV. Equataion (2) is used to fit the data iteratively and get the converged dressed cross sections, during that the cross section line shape is similar to the one in Fig. 2(a). Other two different lineshapes with comparable fitting goodness, that are similar to the results shown in Figs. 2(b) and 2(c), plus an additional lineshape obtained by the LOWESS (LOcally WEighted Scatterplot Smoothing) [52,53], are used to calculate the systematic uncertainties for the lineshape description by repeating the iterations and taking the differences in the results. The systematic uncertainty of the measured $E_{\mathrm{c.m.}}$ is found to be less than 0.8 (0.6 MeV) for $4.226 < E_{\mathrm{c.m.}} < 4.6$ $(4.6 < E_{\mathrm{c.m.}} < 4.95$ GeV) [25–27] and it is used to shift all the energy points to conservatively estimate the impacts on the measured cross sections. Since the cross section lineshape varies dramatically near the threshold, the $E_{\mathrm{c.m.}}$ uncertainty could have significant impact on the ISR correction factors nearby, subsequently affecting the measured cross sections and the fitting results around the threshold. The MC samples at the first four $E_{\mathrm{c.m.}}$ points near the threshold are regenerated with the shifted energies to update ISR corrections. After the iterations with the shifted energy points and the updated ISR correction factors near threshold, the resulting differences in the Born cross sections are taken as the systematic uncertainties due to the $E_{\mathrm{c.m.}}$ uncertainty. These systematic uncertainties are summarized in Table II by assuming no correlation among different sources.

The sum of three BW amplitudes with the one for the phase-space is an imperfect model, but it is useful to describe the cross section line shape smoothly for the iterative ISR correction procedure and to obtain masses and

TABLE II. Relative systematic uncertainties of the measured Born cross sections. As the effects and the data statistics are energy dependent, some systematic uncertainties are estimated in several energy intervals combining some datasets with low luminosities.

<table>
<tr><th>Sources</th><th colspan="9">Systematic uncertainties (%)</th></tr>
<tr><td>Common</td><td colspan="9">4.0</td></tr>
<tr><td>Energy (interval) (GeV)</td><td>4.226</td><td>4.228</td><td>4.233</td><td>4.233 ∼ 4.24</td><td>4.24 ∼ 4.3</td><td>4.3 ∼ 4.4</td><td>4.4 ∼ 4.82</td><td>4.843</td><td>4.86 ∼ 4.95</td></tr>
<tr><td>Signal yields fitting with fixed parameters</td><td colspan="5">2.0</td><td>5.0</td><td colspan="3">2.0</td></tr>
<tr><td>Signal yields fitting range</td><td colspan="5">4.0</td><td>5.0</td><td colspan="3">4.0</td></tr>
<tr><td>Cross section line shape description</td><td colspan="4">5.0</td><td>2.0</td><td>5.0</td><td>2.0</td><td>5.0</td><td>2.0</td></tr>
<tr><td>$E_{\mathrm{c.m.}}$ uncertainty</td><td>24.5</td><td>20.0</td><td>9.4</td><td colspan="6">0.8</td></tr>
<tr><td>Total</td><td>25.7</td><td>21.5</td><td>12.2</td><td>7.9</td><td>6.4</td><td>9.6</td><td>6.4</td><td>7.9</td><td>6.4</td></tr>
</table>

TABLE III. The systematic uncertainties of the fitted masses and widths. Fitting represent the uncertainty from the multiple fitting results. R represent the uncertainty from the barrier radius, $E_{\mathrm{c.m.}}$ the systematic errors from the $E_{\mathrm{c.m.}}$ uncertainty and the $\sigma_{\mathrm{dressed}}$ the systematic uncertainties on the measured dressed cross sections.

Sources	Fitting	R	$E_{\mathrm{c.m.}}$	$\sigma_{\mathrm{dressed}}$	Total
M_1 (MeV/c^2)	8.8	2.9	28.3	5.1	30
Γ_1 (MeV)	6.7	1.9	51	11.8	53
M_2 (MeV/c^2)	3.5	0.6	4.0	3.0	6.1
Γ_2 (MeV)	2.6	0.2	7.6	1.0	8.1
M_3 (MeV/c^2)	7.3	1.0	2.4	5.1	9.3
Γ_3 (MeV)	32.9	1.1	5.3	3.4	34

widths of the resonance(-like) structures for reference. The systematic uncertainties of the fitted masses and widths of the three resonances are listed in Table III. There are three fitting results as listed in Table I with comparable goodness of fit. The fitting result 1 is taken as the nominal one, and the biggest differences in the fitted central values between result 1 and the other two are taken as the systematic uncertainties from the multiple fitting results. The parameter R is changed from 1.6 in the nominal fit to 5 GeV^{-1} (corresponds the scale of the strong interaction which is about 1 fm) [47,54], and the variations in the fitting results are taken as the corresponding systematic uncertainties. The uncertainty from the measured $E_{\mathrm{c.m.}}$ has impact not only on the cross sections but also on the fitting results. After the iterations with the shifted energies and the updated ISR correction factors, the differences in the fitting results are considered as the uncertainty from the $E_{\mathrm{c.m.}}$ uncertainty. The systematic uncertainties on the measured dressed cross sections, which are considered as the same as these on the Born cross sections since the uncertainty from VP correction is negligible, consist of a common part and an uncommon part. The common part is the same for all energies and has no effect on fitted masses and widths of the BW functions. The uncommon part is included to redo the cross section fitting and the resulting differences are taken as systematic uncertainties.

In summary, with the world's largest e^+e^- scan data sample between 4.226 and 4.95 GeV accumulated by BESIII, the Born cross sections of $e^+e^- \to D_s^{*+}D_s^{*-}$ are measured precisely. Two enhancements in the $E_{\mathrm{c.m.}}$ dependent cross sections are observed around 4.2 and 4.45 GeV. The $E_{\mathrm{c.m.}}$ dependent cross section lineshape is modeled with a sum of three BW and one PHSP amplitudes. The fitted mass and width for the first resonance are $(4186.8 \pm 8.7 \pm 30)$ MeV/c^2 and $(55 \pm 15 \pm 53)$ MeV, respectively. These results are consistent with the $\psi(4160)$ observed in the inclusive cross section of $e^+e^- \to$ hadrons [55] and in the dimuon spectrum of $B^- \to K^-\mu^+\mu^-$ [56]. While considering the systematic uncertainties, these results are also consistent with $\psi(4230)$ observed in the $\pi^+\pi^-J/\psi$ mode. The fitted mass and width for the second resonance are $(4414.6 \pm 3.4 \pm 6.1)$ MeV/c^2 and $(122.5 \pm 7.5 \pm 8.1)$ MeV, respectively. The mass is consistent with $\psi(4415)$, and the measured width from this work is a bit higher than the world average value of $\psi(4415)$ [35], but still within three standard deviations. If we assume that this resonance is the $\psi(4415)$, this is the first time that this state is observed in the $D_s^{*+}D_s^{*-}$ decay mode. An additional third BW amplitude describes the $E_{\mathrm{c.m.}}$ dependent cross sections around 4.79 GeV better than just using two BW functions, with statistical significance greater than 5.9σ, however, more data points in the vicinity are needed for further clarification [57]. It is out of the scope of this Letter, but a unitary approach based on K-matrix formalism to fit the cross-section results of various exclusive channels is expected to be carried out as a more comprehensive and robust analysis of the vector-charmonium(-like) structures (for instance, an analysis for vector bottomonia with this method can be found in Ref. [58]).

The BESIII Collaboration thanks the staff of BEPCII and the IHEP computing center for their strong support. This work is supported in part by National Key R&D Program of China under Contracts No. 2020YFA0406300, No. 2020YFA0406400; National Natural Science Foundation of China (NSFC) under Contracts No. 12150004, No. 11635010, No. 11735014, No. 11835012, No. 11935015, No. 11935016, No. 11935018, No. 11961141012, No. 12022510, No. 12025502, No. 12035009, No. 12035013, No. 12061131003, No. 12192260, No. 12192261, No. 12192262, No. 12192263, No. 12192264, No. 12192265, No. 12221005, No. 12225509, No. 12235017, No. U1732105, No. U1632106; Program of Science and Technology Development Plan of Jilin Province of China under Contract No. 20210508047RQ; The Fundamental Research Funds of Shandong University; the Chinese Academy of Sciences (CAS) Large-Scale Scientific Facility Program; the CAS Center for Excellence in Particle Physics (CCEPP); CAS Key Research Program of Frontier Sciences under Contracts No. QYZDJ-SSW-SLH003, No. QYZDJ-SSW-SLH040; 100 Talents Program of CAS; The Institute of Nuclear and Particle Physics (INPAC) and Shanghai Key Laboratory for Particle Physics and Cosmology; ERC under Contract No. 758462; European Union's Horizon 2020 research and innovation programme under Marie Sklodowska-Curie grant agreement under Contract No. 894790; German Research Foundation DFG under Contracts No. 443159800, No. 455635585, Collaborative Research Center CRC 1044, FOR5327, GRK 2149; Istituto Nazionale di Fisica Nucleare, Italy; Ministry of Development of Turkey under Contract No. DPT2006K-120470; National Research Foundation of Korea under

Contract No. NRF-2022R1A2C1092335; National Science and Technology fund of Mongolia; National Science Research and Innovation Fund (NSRF) via the Program Management Unit for Human Resources & Institutional Development, Research and Innovation of Thailand under Contract No. B16F640076; Polish National Science Centre under Contract No. 2019/35/O/ST2/02907; The Swedish Research Council; U.S. Department of Energy under Contract No. DE-FG02-05ER41374.

[a]Also at the Moscow Institute of Physics and Technology, Moscow 141700, Russia.
[b]Also at the Novosibirsk State University, Novosibirsk, 630090, Russia.
[c]Also at the NRC "Kurchatov Institute", PNPI, 188300, Gatchina, Russia.
[d]Also at Goethe University Frankfurt, 60323 Frankfurt am Main, Germany.
[e]Also at Key Laboratory for Particle Physics, Astrophysics and Cosmology, Ministry of Education; Shanghai Key Laboratory for Particle Physics and Cosmology; Institute of Nuclear and Particle Physics, Shanghai 200240, People's Republic of China.
[f]Also at Key Laboratory of Nuclear Physics and Ion-beam Application (MOE) and Institute of Modern Physics, Fudan University, Shanghai 200443, People's Republic of China.
[g]Also at State Key Laboratory of Nuclear Physics and Technology, Peking University, Beijing 100871, People's Republic of China.
[h]Also at School of Physics and Electronics, Hunan University, Changsha 410082, China.
[i]Also at Guangdong Provincial Key Laboratory of Nuclear Science, Institute of Quantum Matter, South China Normal University, Guangzhou 510006, China.
[j]Also at Frontiers Science Center for Rare Isotopes, Lanzhou University, Lanzhou 730000, People's Republic of China.
[k]Also at Lanzhou Center for Theoretical Physics, Lanzhou University, Lanzhou 730000, People's Republic of China.
[l]Also at the Department of Mathematical Sciences, IBA, Karachi 75270, Pakistan.

[1] B. Aubert *et al.* (*BABAR* Collaboration), Phys. Rev. Lett. **95**, 142001 (2005).
[2] C. Z. Yuan *et al.* (Belle Collaboration), Phys. Rev. Lett. **99**, 182004 (2007).
[3] X. L. Wang *et al.* (Belle Collaboration), Phys. Rev. Lett. **99**, 142002 (2007).
[4] J. P. Lees *et al.* (*BABAR* Collaboration), Phys. Rev. D **89**, 111103(R) (2014).
[5] M. Ablikim *et al.* (BESIII Collaboration), Phys. Rev. Lett. **118**, 092001 (2017).
[6] C. P. Shen *et al.* (Belle Collaboration), Phys. Rev. D **89**, 072015 (2014).
[7] M. Ablikim *et al.* (BESIII Collaboration), Phys. Rev. D **97**, 071101 (2018).
[8] X. L. Wang *et al.* (Belle Collaboration), Phys. Rev. D **87**, 051101 (2013).
[9] M. Ablikim *et al.* (BESIII Collaboration), Phys. Rev. D **91**, 112005 (2015).
[10] M. Ablikim *et al.* (BESIII Collaboration), Phys. Rev. D **94**, 032009 (2016).
[11] M. Ablikim *et al.* (BESIII Collaboration), Phys. Rev. Lett. **111**, 242001 (2013).
[12] M. Ablikim *et al.* (BESIII Collaboration), Phys. Rev. Lett. **113**, 212002 (2014).
[13] M. Ablikim *et al.* (BESIII Collaboration), Phys. Rev. Lett. **118**, 092002 (2017).
[14] M. Ablikim *et al.* (BESIII Collaboration), Phys. Rev. D **104**, 052012 (2021).
[15] M. Ablikim *et al.* (BESIII Collaboration), Phys. Rev. Lett. **114**, 092003 (2015).
[16] B. Aubert *et al.* (*BABAR* Collaboration), Phys. Rev. D **76**, 111105 (2007).
[17] G. Pakhlova *et al.* (Belle Collaboration), Phys. Rev. D **77**, 011103 (2008).
[18] M. Ablikim *et al.* (BESIII Collaboration), Phys. Rev. Lett. **130**, 121901 (2023).
[19] M. Ablikim *et al.* (BESIII Collaboration), Phys. Rev. Lett. **122**, 102002 (2019).
[20] D. Cronin-Hennessy *et al.* (CLEO Collaboration), Phys. Rev. D **80**, 072001 (2009).
[21] P. del Amo Sanchez *et al.* (*BABAR* Collaboration), Phys. Rev. D **82**, 052004 (2010).
[22] G. Pakhlova *et al.* (Belle Collaboration), Phys. Rev. D **83**, 011101(R) (2011).
[23] M. Ablikim *et al.* (BESIII Collaboration), Nucl. Instrum. Methods Phys. Res., Sect. A **614**, 245 (2010).
[24] K. X. Huang *et al.*, Nucl. Sci. Tech. **33**, 142 (2022).
[25] M. Ablikim *et al.* (BESIII Collaboration), Chin. Phys. C **40**, 063001 (2016).
[26] M. Ablikim *et al.* (BESIII Collaboration), Chin. Phys. C **45**, 103001 (2021).
[27] M. Ablikim *et al.* (BESIII Collaboration), Chin. Phys. C **46**, 113003 (2022).
[28] M. Ablikim *et al.* (BESIII Collaboration), Chin. Phys. C **46**, 113002 (2022).
[29] M. Ablikim *et al.* (BESIII Collaboration), Chin. Phys. C **41**, 063001 (2017).
[30] S. Agostinelli *et al.* (GEANT4 Collaboration), Nucl. Instrum. Methods Phys. Res., Sect. A **506**, 250 (2003).
[31] D. J. Lange, Nucl. Instrum. Methods Phys. Res., Sect. A **462**, 152 (2001).
[32] R. G. Ping, Chin. Phys. C **32**, 599 (2008).
[33] S. Jadach, B. F. L. Ward, and Z. Was, Comput. Phys. Commun. **130**, 260 (2000).
[34] S. Jadach, B. F. L. Ward, and Z. Was, Phys. Rev. D **63**, 113009 (2001).
[35] R. L. Workman *et al.* (Particle Data Group), Prog. Theor. Exp. Phys. **2022**, 083C01 (2022).
[36] J. C. Chen, G. S. Huang, X. R. Qi, D. H. Zhang, and Y. S. Zhu, Phys. Rev. D **62**, 034003 (2000); R. L. Yang, R. G. Ping, and H. Chen, Chin. Phys. Lett. **31**, 061301 (2014).
[37] E. Richter-Was, Phys. Lett. B **303**, 163 (1993).
[38] M. Ablikim *et al.* (BESIII Collaboration), Phys. Rev. D **92**, 092006 (2015).
[39] This is a nominal value and the measured one is $4287.88 \pm 0.06 \pm 0.34$ MeV [26].
[40] A measurement by BESIII to be published in near future.
[41] S. Actis *et al.*, Eur. Phys. J. C **66**, 585 (2010).

[42] W. Y. Sun, T. Liu, M. Q. Jing, L. L. Wang, B. Zhong, and W. M. Song, Front. Phys. **16**, 64501 (2021).
[43] $e^+e^- \to \gamma^*/Y \to D_s^{*+}D_s^{*-}$ is a vector $\to$ vector $+$ vector process, P-parity conservation requires the orbit angular momentum number L of the $D_s^{*+}D_s^{*-}$ system to be odd and $L = 1$ (P wave) is the most likely case.
[44] BW_1 is to describe the cross section enhancement near the threshold. Unlike in $BW_{2,3}$, $\beta^3(M_1)$ is not present in BW_1 so that M_1 can go below the threshold in the fits.
[45] J. M. Blatt and V. F. Weisskopf, Science **117**, 419 (1953).
[46] F. V. Hippel and C. Quigg, Phys. Rev. D **5**, 624 (1972).
[47] L. Y. Alain, L. Jean-Pierre, and R. Patrick, Phys. Rev. D **99**, 073010 (2019).
[48] See Supplemental Material at http://link.aps.org/supplemental/10.1103/PhysRevLett.131.151903 for the detailed information about the Born cross section.
[49] M. Ablikim *et al.* (BESIII Collaboration), Phys. Rev. D **104**, 012016 (2015).
[50] M. Ablikim *et al.* (BESIII Collaboration), Phys. Rev. D **81**, 052005 (2010).
[51] M. Ablikim *et al.* (BESIII Collaboration), Chin. Phys. C **39**, 093001 (2015).
[52] W. S. Cleveland, J. Am. Stat. Assoc. **74**, 829 (1979).
[53] W. S. Cleveland and S. J. Devlin, J. Am. Stat. Assoc. **83**, 596 (1988).
[54] M. Mikhasenko *et al.*, Eur. Phys. J. C **78**, 727 (2018).
[55] M. Ablikim *et al.* (BESII Collaboration), Phys. Lett. B **660**, 315 (2008).
[56] R. Aaij *et al.* (LHCb Collaboration), Phys. Rev. Lett. **111**, 112003 (2013).
[57] M. Ablikim *et al.* (BESIII Collaboration), Chin. Phys. C **44**, 040001 (2020).
[58] N. Hüsken, R. E. Mitchell, and E. S. Swanson, Phys. Rev. D **106**, 094013 (2022).